ACS OMEGA

http://pubs.acs.org/journal/acsodf

Article

Controlling the Hydrogen Generation Reaction from Waste Water in Oil Fields Using an Ionic Liquid

Mohamed A. Deyab* and Mohsen Mohammed Al Qhatani

Cite This: *ACS Omega* 2023, 8, 4337−4343

Read Online

ACCESS | Metrics & More | Article Recommendations

ABSTRACT: Hydrogen production technologies are attracting widespread interest in energy technologies. The conventional methods for hydrogen production suffer from high cost, restricting their production everywhere. Here, we use waste formation water from a petroleum field and carbon steel materials to produce hydrogen. The most suitable conditions have been investigated to maximize the hydrogen yield. In addition, an ionic liquid (i.e., tributylmethylammonium methyl carbonate, BMAMC) has been used to control the hydrogen generation reaction. We reveal that the amount of hydrogen release rapidly increases with decreasing pH of the solution from 6.7 to 2.5. A further increase in temperature resulted in more amount of hydrogen release. Our study investigates the influence of chloride ions on hydrogen generation activity. The results revealed that ionic liquid BMAMC remarkably decreases the amount of hydrogen release with an efficiency of 92% at 5.08 × 10^{-4} M. The addition of ionic liquid BMAMC into waste formation water increases the activation energy of the hydrogen generation reaction. The Langmuir model is the best isotherm describing the adsorption of BMAMC on carbon steel. Finally, to confirm the adsorption of the ionic liquid BMAMC, scanning electron microscopy and Fourier-transform infrared spectroscopy analysis were conducted.

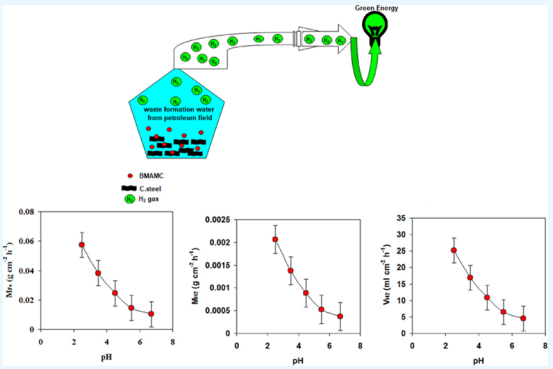

1. INTRODUCTION

Now, hydrogen energy is a promising source for energy in modern industrials and vehicles. Hydrogen has four essential benefits: very clean, sustainable, high energy content, and multiple uses.[1,2] At present, large mass production is mostly obtained from fossil fuel sources.[3] Although this source gives large quantities, it is a danger to the environment; in addition, it is a depleted and costly source.[4]

Recently, many studies have focused on water electrolysis to generate hydrogen energy. However, one of the main disadvantages of this method is the use of electricity to complete the electrolysis process, and this increases the cost of producing hydrogen; in addition, electricity is not available anywhere.[5] The alternative approach to produce hydrogen depends on hydrogen storage materials such as metal hydride[6] and chemical hydride.[7] This approach also is restricted because of the high cost of these hydride materials.

The modern methods use hydrogen production in which the electrochemical reactions occur during the immersion of some metal in solutions.[8] The most common metal used in this method is aluminum in aqueous alkaline environments.[9] The main problem here is the formation of an oxide layer on the surface of the metal, which stops the hydrogen generation reactions.[10]

Increasing reports toward solving this problem suggest that we can use aluminum alloys. For instance, Katsoufis et al.[11] indicated that the use of aluminum alloys such as Al-6061 leads to the generation of more hydrogen than pure aluminum. Recently, some metals such as Fe, Sn, and Ni alloys[12−14] have been used for hydrogen generation. However, their high cost is still a great challenge.

Here, we face two main challenges. The first is the cost of materials used to generate hydrogen. The second is the deposition of corrosion products on the metal surface, which stops the hydrogen generation reaction.

To address these challenges, we aim to use waste formation water from a petroleum field and carbon steel materials to generate hydrogen. The low cost of waste formation water and carbon steel materials make the utilization of these materials as a hydrogen source a promising strategy. In general, waste formation water is rich in high salt content and this leads to continuous hydrogen generation reactions. Here, we will design the most suitable conditions that allow obtaining a high hydrogen yield. In addition, an ionic liquid (i.e., tributylme-

Received: December 1, 2022
Accepted: December 30, 2022
Published: January 13, 2023

thylammonium methyl carbonate, BMAMC) will be tested as an inhibitor for the hydrogen generation reaction. Thermodynamic quantities and adsorption discussion on the ionic liquid and carbon steel interaction will be addressed.

2. EXPERIMENTAL SECTION

2.1. Materials. Carbon steel materials were obtained from a waste petroleum pipeline. The chemical composition of this material was detected using X-ray fluorescence spectroscopy (SPECTRO Analytical Instruments GmbH). According to this method, the carbon steel composition is 0.32% C, 0.23% Mg, 0.28% Si, 0.023% P, 0.02% S, 0.12% Ni, and remaining % Fe.

The waste formation water was collected from petroleum wells (Egypt). The chemical and physical analysis of waste water is presented in Table 1. The ionic liquid BMAMC (see Figure 1) was provided by Sigma-Aldrich.

Table 1. Chemical and Physical Analysis of Waste Formation Water

total dissolved solids (T.D.S.)	200154.2 mg/L
salinity (as NaCl)	202451.1 mg/L
alkalinity (as $CaCO_3$)	16.7 mg/L
total hardness (as $CaCO_3$)	70231.5 mg/L
density @ 25 °C	1.14340 g/mL
specific gravity	1.14453
pH @ 25 °C	6.5
conductivity	21.8 × 10^{-2} mohs/cm @28 °C
Inorganic Chemical Constituents—Cation	
lithium	7.09 mg/L
sodium	47444.14 mg/L
ammonium	Nil
potassium	774.01 mg/L
magnesium	1064.98 mg/L
calcium	26370.00 mg/L
strontium	Nil
barium	Nil
Inorganic Chemical Constituents—Anion	
fluoride	145.22 mg/L
chloride	122697.64 mg/L
bromide	1353.13 mg/L
nitrate	76.96 mg/L
nitrite	nil
sulfate	200.70 mg/L
hydroxide	nil
carbonate	nil
bicarbonate	20.3 mg/L

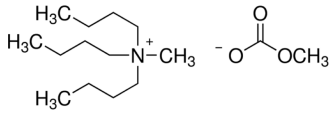

Figure 1. Molecular structure of BMAMC solution.

2.2. H_2 Evolution Assessments. The carbon steel specimen (dimension 2.49 × 1.48 × 0.2 cm) was immersed in the 100 mL waste formation water for 12 h at different pH and temperatures. Prior to each experiment, the specimens were cleaned according to the standard method (ASTM-B322-99-2014) and ASTM G1-03.[15,16]

The volume of H_2 evolution during the reaction was illustrated in earlier studies.[17] To estimate the rate of hydrogen generation (V_{H2}) during the immersion, we have computed the carbon steel surface area (A) and immersion time (t), which are related to the following relation:[17]

$$V_{H2} = \text{volume of } H_2 \text{ evolution (ml)}/A\ (\text{cm}^2) \times t\ (\text{h}) \quad (1)$$

The mass loss of carbon steel during the H_2 evolution reaction was measured according to the standard method (ASTM-G1/90-2000).[18] To estimate the rate of mass loss of carbon steel (M_{Fe}) during the immersion, we have computed the carbon steel surface area (A) and immersion time (t), which are related to the following relation:[19]

$$M_{Fe} = \text{mass loss of carbon steel (g)}/A\ (\text{cm}^2) \times t\ (\text{h}) \quad (2)$$

By using M_{Fe}, the amount of H_2 evolution (M_{H2}) was calculated using the following relation:

$$M_{H2} = [(M_{Fe} \times \text{number of electrons lost}) /(\text{atomic mass of iron})] \quad (3)$$

To adjust solution pH, we added some of the drops of aqueous solutions of HCl or NaOH to waste formation water.

To investigate the purity of H_2 evolution, the component of the gas released during the carbon steel immersion in waste formation water was analyzed using a gas chromatograph (GC-2014, Shimadzu Corporation, Japan). ASTM D2504 was used as the standard method. All experiments were run three times to verify the accuracy of the data.

2.3. Electrochemical Measurements. The cathodic polarization curve was recoded using a potentioscan (model: Gamry's Reference-3000). In this system, we used a three electrode cell (i.e., carbon steel electrode, Pt electrode, and calomel electrode). The polarization curves were recoded with a scan rate of 1.25 mV s^{-1}. In this study, the carbon steel electrode has a cylindrical shape with an exposed area equal to 0.543 cm^2.

2.4. Surface Characterization. Selected samples were analyzed by scanning electron microscopy (SEM) (JEOL, Quantek detector) to inspect the morphology of the carbon steel surface after some experiments. In addition, the Fourier-transform infrared (FTIR) spectroscopy analysis was conducted for pure ionic liquid BMAMC and the surface product using an FTIR instrument (ATI Mattson Infinity Series, USA).

3. RESULTS AND DISCUSSION

3.1. pH and Temperature Influences. In this section, the influences of solution pH and the changes in the environment temperatures on the amount of hydrogen released from the reaction of carbon steel with waste formation water are discussed in detail. Generally, the amount of both hydrogen release (i.e., V_{H2} and M_{H2}) and mass loss of carbon steel (i.e., M_{Fe}) rapidly increases with decreasing pH of the solution from 6.7 to 2.5 (see Figure 2).

The hydrogen release rate due to the reaction of waste formation water with carbon steel on the anodic and cathodic sites is expressed as follows:[20]

$$Fe \rightarrow Fe^{2+} + 2e\ (\text{anodic site, mass loss}) \quad (4)$$

$$Fe + H_3O^+ \rightarrow Fe(H_3O^+)_{ads}\ (\text{cathodic site}) \quad (5)$$

$$Fe(H_3O^+)_{ads} + e \rightarrow Fe(H_3O)_{ads}\ (\text{cathodic site}) \quad (6)$$

https://doi.org/10.1021/acsomega.2c07685
ACS Omega 2023, 8, 4337−4343

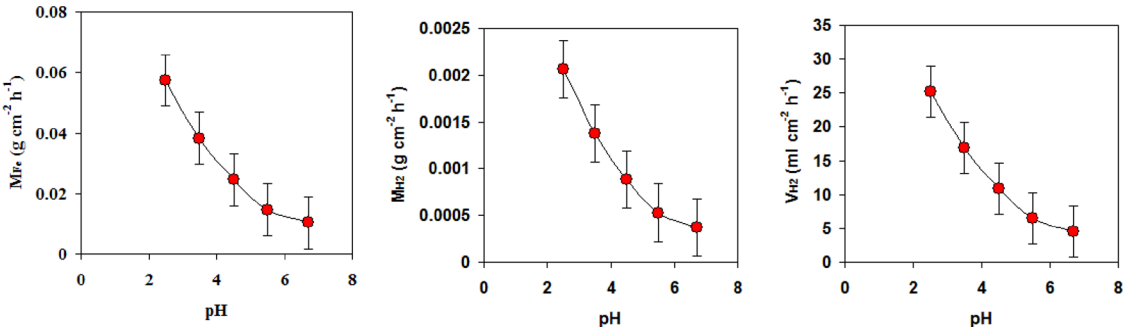

Figure 2. Amount of hydrogen released (V_{H2} and M_{H2}) and mass loss of carbon steel (M_{Fe}) during the reaction of carbon steel with waste formation water at different pH.

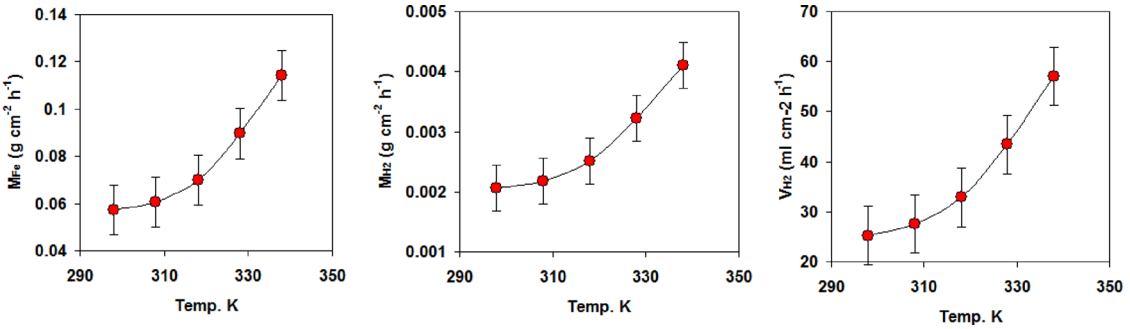

Figure 3. Amount of hydrogen released (V_{H2} and M_{H2}) and mass loss of carbon steel (M_{Fe}) during the reaction of carbon steel with waste formation water (pH 2.5) at different temperatures.

$$Fe(H_3O)_{ads} + H_3O^+ + e \rightarrow Fe + 2H_2O + H_2 \uparrow \text{(cathodic site, } H_2 \text{ release)} \quad (7)$$

The presence of chlorides ions in waste formation water leads to the continuous carbon steel dissolution and hydrogen release during the anodic and cathodic processes, which is responsible for the high amount of hydrogen release.[21,22] We list the following reactions in order to more clearly understand the part of chloride ions in the ongoing anodic and cathodic reactions and in preventing the creation of the oxide layer on the surface of the metal:[22]

$$Fe + Cl^- \rightarrow Fe\cdots Cl^- \quad (8)$$

$$Fe\cdots Cl^- + Fe\cdots OH \rightarrow 2e + Fe + FeOH^+ + Cl^- \quad (9)$$

$$FeOH^+ + H^+ \rightarrow Fe^{2+} + H_2O \quad (10)$$

$$Fe + 2Cl^- \rightarrow FeCl_2 + 2e \quad (11)$$

According to the above reactions, the solubility of $FeCl_2$ compound in the solution increases with decreasing pH of the solution.

This suggests that the lower pH facilitates the cathodic reaction and will lead to more hydrogen release.

At low pH (i.e., 2.5), we also tested the influences of the temperature increase on the amount of hydrogen release. Under these conditions, we noted that the amount of both hydrogen release (i.e., V_{H2} and M_{H2}) and mass loss of carbon steel (i.e., M_{Fe}) rapidly increases with increasing temperature from 298 to 338 K (see Figure 3). In this case, the temperature rise causes an increase in both mass loss and hydrogen release reactions. To accelerate the hydrogen release reaction, we need to increase the activated ions with energy more than the activation energy of the hydrogen release reaction. This effect has occurred through the increasing temperature.[23,24]

To check the purity of hydrogen released from the reaction of carbon steel and waste formation water, the releasing gas from this reaction was detected by gas chromatography. As illustrated in the chromatogram (Figure 4), the sharp signal at 0.72 s (retention time) corresponds to hydrogen gas.[25] From the calculated area under the peak, we found that the purity of hydrogen is about 99.8%.

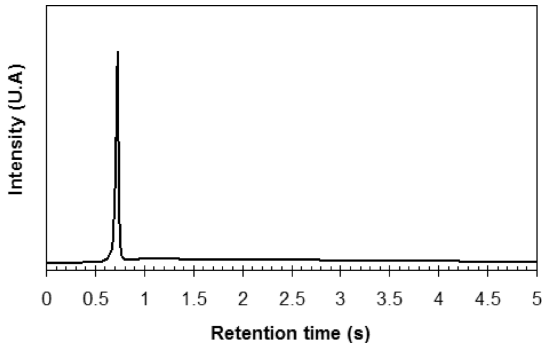

Figure 4. Gas chromatogram recorded during the reaction of carbon steel with waste formation water (pH 2.5) at 298 K.

To support these data, the cathodic polarization experiments were conducted in the case of the immersion of carbon steel in waste formation water at different pH and temperatures. Notably, the cathodic current density increases with decreasing pH of the solution from 6.7 to 2.5 (see Figure 5).

This means that the amount of hydrogen release increases in more acidic solution. At the same time, we noted that the cathodic current density rapidly increases with increasing

https://doi.org/10.1021/acsomega.2c07685
ACS Omega 2023, 8, 4337−4343

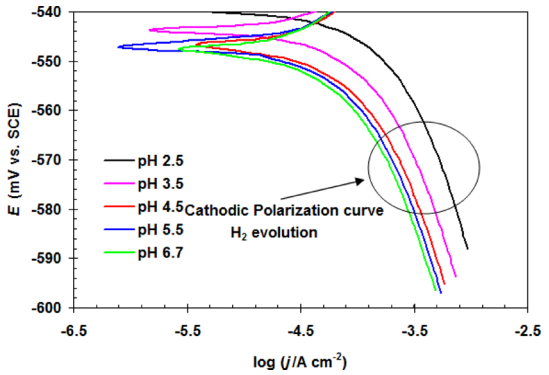

Figure 5. Cathodic polarization curves of carbon steel in waste formation water at different pH.

temperature from 298 to 338 K (see Figure 6). These results suggest that the pH and temperature have a great role in the

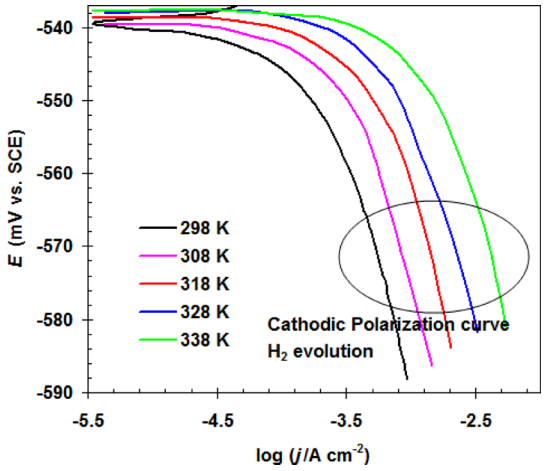

Figure 6. Cathodic polarization curves of carbon steel in waste formation water (pH 2.5) at different temperatures.

increase of the amount of hydrogen release during the immersion of carbon steel and waste formation water.

3.2. Effect of BMAMC on the Hydrogen Release. In this section, the role of BMAMC on the control of the hydrogen released during the immersion of carbon steel in waste formation water at pH 2.5 and 298 K was investigated. The efficiency of ionic liquid (η_{H2}%) and the rates of hydrogen generation (V_{H2}) in the presence of BMAMC were collected and are listed in Table 2. The η_{H2}% can be formulated as:[26]

$$\eta_{H_2}\% = [(V^0{}_{H2} - V_{H2})/(V^0{}_{H2})] \times 100 \quad (12)$$

where $V^0{}_{H2}$ is the rate of hydrogen generation in the absence of BMAMC. It is noted that the addition of BMAMC in waste formation water leads to the slowdown in the rates of hydrogen generation (see Table 2). In addition, the high concentration of BMAMC further deteriorates the level of hydrogen generation.

It is significant to highlight that a considerable increase in the η_{H2}% value (92.0%) occurs at 5.08×10^{-4} M of BMAMC.

An additional inspection into the efficiency of ionic liquid BMAMC comes from the cathodic polarization curve (see Figure 7). It is observed that the cathodic current density rapidly decreases with increasing the BMAMC concentration from 0.72×10^{-4} M to 5.08×10^{-4} M (see Figure 7).

Table 2. Rate of Hydrogen Generation (V_{H2}) and the Corresponding Efficiency of Ionic Liquid (η_{H2}%) during the Reaction of Carbon Steel with Waste Formation Water (pH 2.5) without and with Different Concentrations of Ionic Liquid BMAMC at 298 K

conc. BMAMC (M)	V_{H2} (ml cm^{-2} h^{-1})	η_{H2}%
waste formation water	25.25 ± 0.65	
0.72×10^{-4}	17.07 ± 0.52	32.3
1.45×10^{-4}	11.21 ± 0.63	55.6
2.17×10^{-4}	9.44 ± 0.42	62.6
2.90×10^{-4}	6.08 ± 0.23	75.9
3.63×10^{-4}	4.14 ± 0.21	83.6
4.35×10^{-4}	2.17 ± 0.18	91.4
5.08×10^{-4}	2.02 ± 0.09	92.0

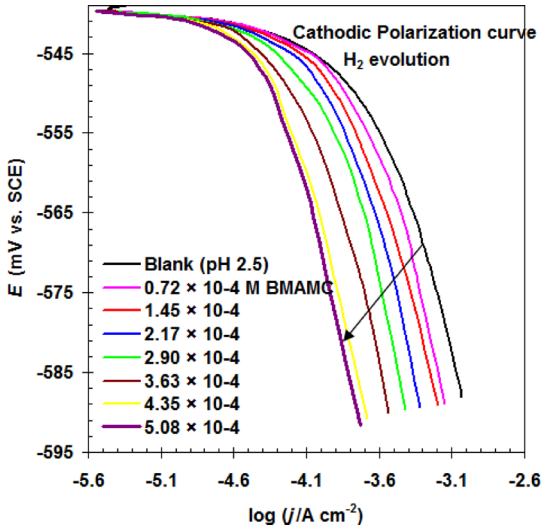

Figure 7. Cathodic polarization curves of carbon steel in waste formation water (pH 2.5) without and with different concentrations of ionic liquid BMAMC at 298 K.

This result confirms that the ionic liquid BMAMC plays a great role in the decreasing of the amount of hydrogen release during the immersion of carbon steel and waste formation water.

The insight on how the ionic liquid inhibits the hydrogen generation comes from the created charges on both the carbon steel surface and ionic liquid molecules. Notably, the carbon steel in the acidic waste formation water carries a positive charge.[27,28] This attracts the negative portion of BMAMC molecules to the carbon steel surface. According to this situation, the cationic portion of BMAMC molecules will be adsorbed on the negative charge sites of carbon steel by Van der Waals to prevent the adsorption of H_3O^+.[15,29−31] These adsorbed ionic liquid BMAMC molecules on the carbon steel surface inhibit the hydrogen generation reaction.

3.3. Thermodynamic and Adsorption Studies. At present, research on the activation energy of the hydrogen generation reaction (E_{aH}) is very significant, which can be investigated from the estimated rate of hydrogen generation V_{H2} in the absence and presence of BMAMC at different temperatures (298−338 K) (see Table 3).

It is discovered that the rates of hydrogen generation V_{H2} in both blank and inhibited waste formation water are slightly increased by increasing temperatures. This is primarily related to the de-sorption of some BMAMC molecules from the

https://doi.org/10.1021/acsomega.2c07685
ACS Omega 2023, 8, 4337−4343

Table 3. Rate of Hydrogen Generation (V_{H2}) and the Corresponding Efficiency of Ionic Liquid (η_{H2}%) during the Reaction of Carbon Steel with Waste Formation Water (pH 2.5) without (Blank) and with Ionic Liquid BMAMC at Different Temperatures

temp. (K)	V_{H2} (ml cm^{-2} h^{-1}) blank	V_{H2} (ml cm^{-2} h^{-1}) BMAMC (5.08 × 10^{-4} M)	η_{H2}%
298	25.25 ± 0.65	2.02 ± 0.09	92.0
308	27.58 ± 0.68	2.97 ± 0.15	89.2
318	32.84 ± 0.70	4.43 ± 0.19	86.5
328	43.44 ± 0.75	6.64 ± 0.23	84.7
338	57.04 ± 1.02	12.20 ± 0.42	78.6

carbon steel surface because of the high temperature.[32] At the same time, the high temperature accelerates the hydrogen generation reaction.[33,34]

The activation energy of hydrogen generation reaction E_{aH} could be calculated by Arrhenius formula:[32]

$$V_{H2} = A \exp(-E_{aH}/RT) \quad (13)$$

where R = ideal-gas constant, A = Arrhenius constant, and T = absolute temperature.

Figure 8 shows the Arrhenius plots in the absence (blank) and presence of 5.08 × 10^{-4} M of BMAMC.

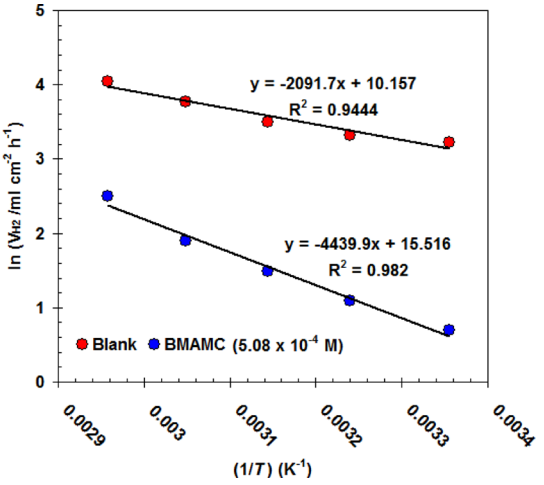

Figure 8. Arrhenius plots in the absence (blank) and presence of 5.08 × 10^{-4} M of BMAMC.

The E_{aH} could be calculated from the slopes of Arrhenius plots. It could be noted that the addition of 5.08 × 10^{-4} M of BMAMC in waste formation water could increase the E_{aH} from 17.35 kJ mol^{-1} (in the case of the blank solution) to 36.84 kJ mol^{-1}. This means that the presence of ionic liquid BMAMC increases the amount of the potential barrier that is required for the hydrogen generation reaction and, consequently, the ionic liquid decreases the amount of hydrogen release.[35]

Adsorption behavior of ionic liquid BMAMC on the carbon steel surface is investigated using the following mathematical eqs 14 and 15.[36]

$$C_{IL}/\theta = (1/K_{ads}) + C_{IL} \quad (14)$$

$$\theta = (V^0{}_{H2} - V_{H2})/(V^0{}_{H2}) \quad (15)$$

In this case, eq 14 represents the Langmuir adsorption isotherm, where C_{IL} is the ionic liquid concentration and K_{ads} is the Langmuir isotherm constant. The best isotherm to the adsorption data is presented in Figure 9.

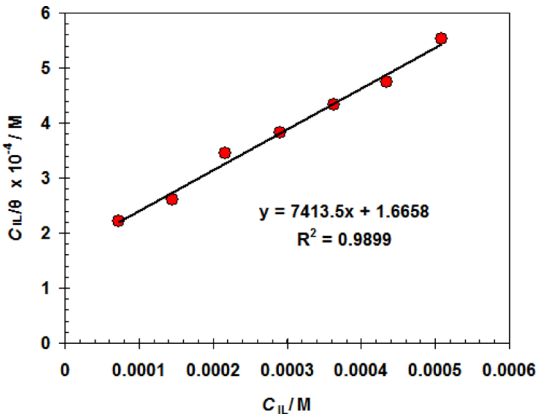

Figure 9. Langmuir adsorption isotherm for carbon steel in waste formation water (pH 2.5) containing increasing concentrations of ionic liquid BMAMC at 298 K.

This figure presents a linear regression of eq 14. We confirm the validity of the Langmuir model because the correlation coefficient (R^2) is close to the unit (R^2 = 0.9899).[37] It is worth noting that the K_{ads} value obtained from Figure 9 was 0.6 × 10^4 M. The high value of K_{ads} refers to the favorable condition for the ionic liquid BMAMC adsorption on the carbon steel surface.[38] The change in standard free energy (ΔG°) can be evaluated from the value of K_{ads} according to eq 16.[39]

$$\Delta G_o = -RT \ln(55.5\ K_{ads}) \quad (16)$$

The value of ΔG° is − 31.45 kJ·mol^{-1}. This means that the adsorption of the BMAMC on the steel surface is spontaneous and belongs to physical adsorption.[39]

3.4. Surface Morphology Studies. Figure 10 shows the surface morphology of carbon steel discovered by SEM after 12 h immersion in waste formation water solution with and without ionic liquid BMAMC. The surface of carbon steel after immersion in waste formation water (Figure 10b) was characterized by a large damage in comparison to the as-received sample (Figure 10a).

According to Figure 10b, the corrosion effects on the carbon steel surface were distributed in a uniform shape. This means that hydrogen generation reactions occur over the whole carbon steel surface. Meanwhile, the corrosion damage by waste formation water was reduced to a high extent after adding 5.08 × 10^{-4} M of ionic liquid BMAMC as seen in Figure 10c.

To confirm the adsorption of the ionic liquid BMAMC on the carbon steel, FTIR analysis was conducted for pure ionic liquid BMAMC and the surface product (see Figure 11). As shown in Figure 11a, hydrogen-bonded O−H stretching occurs at 3420 cm^{-1}, C−H stretch occurs at 3010 cm^{-1}, C═0 stretch occurs at 1730 cm^{-1}, CH_2 bending modes at 1465 cm^{-1}, CH_3 bending absorption at 1375 cm^{-1}, C−N stretching occurs at 1350 cm^{-1}, and C−O stretching occurs at 1150 cm^{-1}. The FT-IR spectrum for the products formed on the carbon steel after immersion in waste formation water containing ionic liquid BMAMC (see Figure 11b) confirms the adsorption of BMAMC on the surface. The shifting in the position of some bands such as hydrogen-bonded O−H, C−O

https://doi.org/10.1021/acsomega.2c07685
ACS Omega 2023, 8, 4337−4343

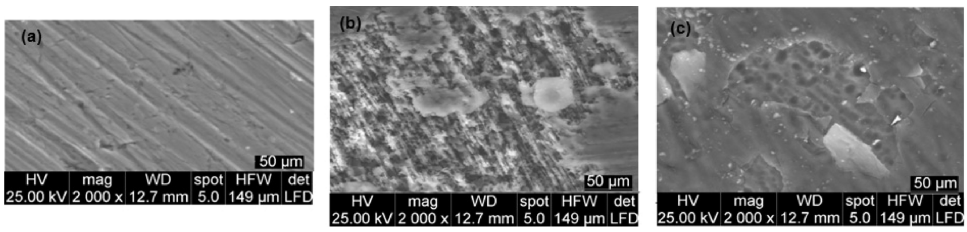

Figure 10. SEM images for (a) abraded carbon steel, (b) carbon steel immersed in waste formation water solution (pH 2.5) at 298 K, (c) carbon steel immersed in waste formation water (pH 2.5) solution containing 4.35×10^{-4} M of ionic liquid BMAMC at 298 K.

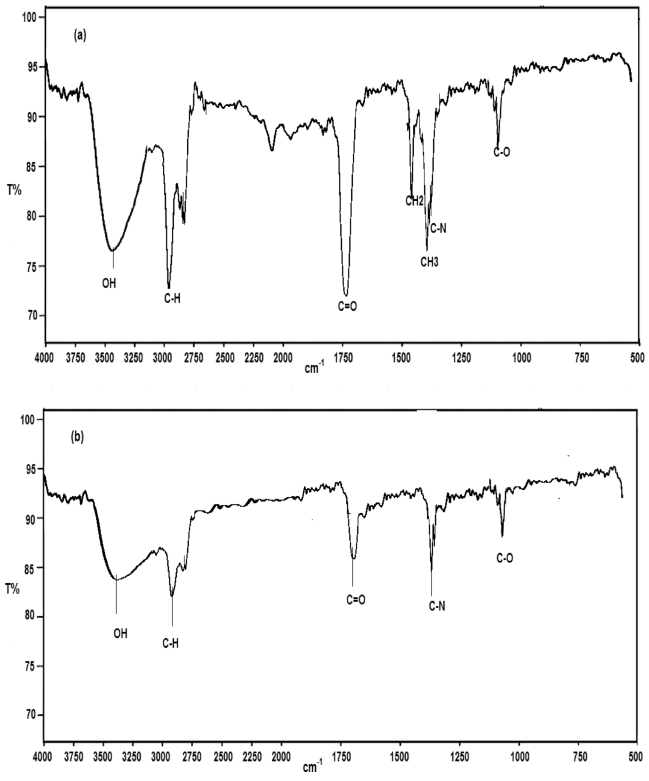

Figure 11. FTIR spectra for pure ionic liquid BMAMC (a) and for the scratched film formed on carbon steel in waste formation water (pH 2.5) solution containing 4.35×10^{-4} M of ionic liquid BMAMC (b).

and C−N indicates the adsorption between the BMAMC molecule and carbon steel.[40−42]

4. CONCLUSIONS

For the first time, the waste formation water from petroleum field and carbon steel is used to generate hydrogen. With the aid of the change in the solution conditions such as pH and temperature, a variety of volumes of H_2 evolution can be obtained. The presence of chloride ions in waste formation water leads to the continuous hydrogen release. It was confirmed that the highest hydrogen release rate (57.04 mL cm^{-2} h^{-1}) could be achieved by immersion carbon steel in waste formation water at pH 2.5 and temperature 338 K. In addition, the introduction of ionic liquid BMAMC with waste formation water could inhibit the hydrogen generation reaction. The performance of ionic liquid is likely due to the adsorption of BMAMC molecules on the carbon steel surface, which is supported by SEM and FTIR inspections. This work reveals the future promise of the waste materials and ionic liquids for the production of hydrogen.

AUTHOR INFORMATION

Corresponding Author

Mohamed A. Deyab − *Egyptian Petroleum Research Institute (EPRI), Cairo 11251, Egypt;* orcid.org/0000-0002-4053-4942; Phone: +201006137150; Email: hamadadeiab@yahoo.com; Fax: + 202 22747433

Author

Mohsen Mohammed Al Qhatani − *Department of Chemistry, College of Sciences, Taif University, Taif 113444, Saudi Arabia*

Complete contact information is available at: https://pubs.acs.org/10.1021/acsomega.2c07685

Notes

The authors declare no competing financial interest.

ACKNOWLEDGMENTS

Taif University Researchers Supporting Project number (TURSP − 2020/19), Taif University, Saudi Arabia. The authors gratefully acknowledge the support of the Science-Technology & Innovation Funding Authority as well as Egyptian Petroleum Research Institute.

REFERENCES

(1) Hanley, E. S.; Deane, J. P.; Gallachoir, B. P. O. The role of hydrogen in low carbon energy futures e a review of existing perspectives. *Renewable Sustainable Energy Rev.* **2018**, *82*, 3027−3045.
(2) Baykara, S. Z. Hydrogen : a brief overview on its sources, production and environmental impact. *Int. J. Hydrogen Energy* **2018**, *43*, 10605−10614.
(3) Ball, M.; Wietschel, M. The future of hydrogen − opportunities and challenges. *Int. J. Hydrogen Energy* **2009**, *34*, 615−627.
(4) Kothari, R.; Buddhi, D.; Sawhney, R. L. Comparison of environmental and economic aspects of various hydrogen production methods. *Renewable Sustainable Energy Rev.* **2008**, *12*, 553−563.
(5) Turner, J.; Sverdrup, G.; Mann, M. K.; Maness, P. C.; Kroposki, B.; Ghirardi, M.; Evans, R. J.; Blake, D. Renewable hydrogen production. *Int. J. Energy Res.* **2008**, *32*, 379−407.
(6) Ouyang, L. Z.; Wen, Y. J.; Xu, Y. J.; Yang, X. S.; Sun, L. X.; Zhu, M. The effect of Ni and Al addition on hydrogen generation of Mg_3La hydride via hydrolysis. *Int. J. Hydrogen Energy* **2010**, *35*, 8161−8165.
(7) Marrero-Alfonso, E. Y.; Beaird, A. M.; Davis, T. A.; Matthews, M. A. Hydrogen generation from chemical hydrides. *Ind. Eng. Chem. Res.* **2009**, *48*, 3703−3712.
(8) Shan, Z.; Liu, Y.; Chen, Z.; Warrender, G.; Tian, J. Amorphous Ni-SMn alloy as hydrogen evolution reaction cathode in alkaline medium. *Int. J. Hydrogen Energy* **2008**, *33*, 28−33.
(9) Wang, H. Z.; Leung, D. Y. C.; Leung, M. K. H.; Ni, M. A review on hydrogen production using aluminum and aluminum alloys. *Renewable Sustainable Energy Rev.* **2009**, *13*, 845−853.
(10) Ho, C.; Huang, C. Enhancement of hydrogen generation using waste aluminum cans hydrolysis in low alkaline de-ionized water. *Int. J. Hydrogen Energy* **2016**, *41*, 3741−3747.

(11) Katsoufis, P.; Doukas, E.; Politis, C.; Avgouropoulos, G.; Lianos, P. Enhanced rate of hydrogen production by corrosion of commercial aluminum. *Int. J. Hydrogen Energy* **2020**, *45*, 10729−10734.
(12) Deyab, M. A. Hydrogen generation during the corrosion of carbon steel in crotonic acid and using some organic surfactants to control hydrogen evolution. *Int. J. Hydrogen Energy* **2013**, *38*, 13511−13519.
(13) Deyab, M. A. Hydrogen generation by tin corrosion in lactic acid solution promoted by sodium perchlorate. *J. Power Sources* **2014**, *268*, 765−770.
(14) Baykara, S. Z. Hydrogen : a brief overview on its sources, production and environmental impact. *Int. J. Hydrogen Energy* **2018**, *43*, 10605−10614.
(15) Deyab, M. A.; Hamdi, N.; Lachkar, M.; El Bali, B. Clay/Phosphate/Epoxy nanocomposites for enhanced coating activity towards corrosion resistance. *Prog. Org. Coat.* **2018**, *123*, 232−237.
(16) Deyab, M. A.; Mele, G. Stainless steel bipolar plate coated with polyaniline/Zn-Porphyrin composites coatings for proton exchange membrane fuel cell. *Sci. Rep.* **2020**, *10*, 3277.
(17) Deyab, M. A. Ionic liquid as an electrolyte additive for high performance lead-acid batteries. *J. Power Sources* **2018**, *390*, 176−180.
(18) ASTM standard designation G1-90: standard practice for preparing, cleaning, and evaluating corrosion test specimens. In: *Annual Book of ASTM Standards, 03.02*, ASTM (Ed.); American Society for Testing and Materials, Washington, D.C.2000, pp. 15−21.
(19) Deyab, M. A.; Ouarsal, R.; Lachkar, M.; El Bali, B.; Essehli, R. *J. Mol. Liq.* **2016**, *219*, 994−999.
(20) El-Taib Heakal, F.; Deyab, M. A.; Osman, M. M.; Nessim, M. I.; Elkholy, A. E. Synthesis and assessment of new cationic Gemini surfactants as inhibitors for carbon steel corrosion in oilfield water. *RSC Adv.* **2017**, *7*, 47335−47352.
(21) Sherif, E.-S. M.; Erasmus, R. M.; Comins, J. D. In situ Raman spectroscopy and electrochemical techniques for studying corrosion and corrosion inhibition of iron in sodium chloride solutions. *Electrochim. Acta* **2010**, *55*, 3657−3663.
(22) Foad El-Sherbini, E. E.; Abd El-Wahab, S. M.; Deyab, M. A. Electrochemical behavior of tin in sodium borate solutions and the effect of halide ions and some inorganic inhibitors. *Corros. Sci.* **2006**, *48*, 1885−1898.
(23) Darwish, N. A.; Hilbert, F.; Lorenz, W. J.; Rosswag, H. The influence of chloride ions on the kinetics of iron dissolution. *Electrochim. Acta* **1973**, *18*, 421−425.
(24) Abd El-Rehim, S. S.; Hassan, H. H.; Deyab, M. A.; Abd El Moneim, A. Experimental and theoretical investigations of adsorption and inhibitive properties of Tween 80 on corrosion of aluminum alloy (A5754) in alkaline media. *Z. Phys. Chem.* **2016**, *230*, 67−78.
(25) Ghareba, S.; Omanovic, S. 12-Aminododecanoic acid as a corrosion inhibitor for carbon steel. *Electrochim. Acta* **2011**, *56*, 3890−3898.
(26) Coronel-Garcıa, M. A.; Salazar-Barrera, J. G.; Malpica-Maldonado, J. J.; Martınez-Salazar, A. L.; Melo-Banda, J. A. J. A. Hydrogen production by aluminum corrosion in aqueous hydrochloric acid solution promoted by sodium molybdate dehydrate. *Int. J. Hydrogen Energy* **2020**, *45*, 13693−13701.
(27) Deyab, M. A.; Fouda, A. S.; Osman, M. M.; Abdel-Fattah, S. Mitigation of acid corrosion on carbon steel by novel pyrazolone derivatives. *RSC Adv.* **2017**, *7*, 45232−45240.
(28) Pope, D. H.; Morris, E. A. Some experiences with microbiologically influenced corrosion. *Mater. Perform.* **1995**, *34*, 23−28.
(29) Deyab, M. A. Efficiency of cationic surfactant as microbial corrosion inhibitor for carbon steel in oilfield saline water. *J. Mol. Liq.* **2018**, *255*, 550−555.
(30) Kannan, P.; Karthikeyan, J.; Murugan, P.; Subba Rao, T.; Rajendran, N. Corrosion inhibition effect of novel methyl benzimidazolium ionic liquid for carbon steel in HCl medium. *J. Mol. Liq.* **2016**, *221*, 368−380.
(31) Moretti, G.; Guidi, F. Tryptophan as copper corrosion inhibitor in 0.5 M aerated sulfuric acid. *Corros. Sci.* **2002**, *44*, 1995−2011.
(32) Moretti, G.; Guidi, F.; Grion, G. Tryptamine as a green iron corrosion inhibitor in 0.5 M deaerated sulphuric acid. *Corros. Sci.* **2004**, *46*, 387−403.
(33) Deyab, M. A. Effects of nonionic surfactant on the parasitic corrosion of lithium anode in lithium−water battery. *RSC Adv.* **2016**, *6*, 32514−32518.
(34) Nessim, M. I.; Zaky, M. T.; Deyab, M. A. Three new gemini ionic liquids: Synthesis, characterizations and anticorrosion applications. *J. Mol. Liq.* **2018**, *266*, 703−710.
(35) Xu, B.; Liu, Y.; Yin, X.; Yang, W.; Chen, Y. Experimental and theoretical study of corrosion inhibition of 3-pyridinecarbozalde thiosemicarbazone for mild steel in hydrochloric acid. *Corros. Sci.* **2013**, *74*, 206−213.
(36) Musa, A. Y.; Kadhum, H.; Mohamad, A. B.; Daud, A. R.; Takriff, M. S.; Kamarudin, S. K. *Corros. Sci.* **2009**, *51*, 2393−2399.
(37) Langmuir, I. The constitution and fundamental properties of solids and liquids. Part 1. Solids. *J. Am. Chem. Soc.* **1916**, *38*, 2221−2295.
(38) Wu, Z.; Yuan, X.; Zhong, H.; et al. Enhanced adsorptive removal of p-nitrophenol from water by aluminum metal−organic framework/reduced graphene oxide composite. *Sci. Rep.* **2016**, *6*, 25638.
(39) Deyab, M. A.; Abd El-Rehim, S. S.; Keera, S. T. Study of the effect of association between anionic surfactant and neutral copolymer on the corrosion behaviour of carbon steel in cyclohexane propionic acid. *Colloids Surf., A* **2009**, *348*, 170−176.
(40) Wijaya, R.; Andersan, G.; Permatasari Santoso, S.; et al. Green Reduction of Graphene Oxide using Kaffir Lime Peel Extract (*Citrus hystrix*) and Its Application as Adsorbent for Methylene Blue. *Sci. Rep.* **2020**, *10*, 667.
(41) Eddy, N. O.; Odoemelam, S. A.; Odiongenyi, A. O. Joint effect of halides and ethanol extract of Lasianthera africana on inhibition of corrosion of mild steel in H_2SO_4. *J. Appl. Electrochem.* **2008**, *39*, 849.
(42) Eddy, N. O.; Ebenso, E. E.; Ibok, U. J. Adsorption, synergistic inhibitive effect and quantum chemical studies of ampicillin (AMP) and halides for the corrosion of mild steel in H_2SO_4. *J. Appl. Electrochem.* **2010**, *40*, 445−456.

https://doi.org/10.1021/acsomega.2c07685
ACS Omega 2023, 8, 4337−4343